AGU ADVANCING EARTH AND SPACE SCIENCES

Geophysical Research Letters

RESEARCH LETTER
10.1029/2023GL106597

Important Role of Low Cloud and Fog in Sulfate Aerosol Formation During Winter Haze Over the North China Plain

Suyi Cai[1,2], Tengyu Liu[1,2,3], Xin Huang[1,2,3], Yu Song[4], Tiantian Wang[4], Zhaobin Sun[5], Jian Gao[6], and Aijun Ding[1,2,3]

[1]Joint International Research Laboratory of Atmospheric and Earth System Sciences, School of Atmospheric Sciences, Nanjing University, Nanjing, China, [2]National Observation and Research Station for Atmospheric Processes and Environmental Change in Yangtze River Delta, Nanjing, China, [3]Frontiers Science Center for Critical Earth Material Cycling, Nanjing University, Nanjing, China, [4]Department of Environmental Science, State Key Joint Laboratory of Environmental Simulation and Pollution Control, Peking University, Beijing, China, [5]State Key Laboratory of Severe Weather, Chinese Academy of Meteorological Sciences, China Meteorological Administration, Beijing, China, [6]Chinese Research Academy of Environmental Sciences, Beijing, China

Key Points:

- High sulfur oxidation ratios under heavy pollution conditions in the North China Plain are associated with low clouds and fog formation
- Sulfate production rates within cloud water can reach 0.5–1.3 μg m^{-3} h^{-1}, with NO_2 and O_3 oxidation pathways dominating
- Vertical mixing of sulfate produced in cloud water to the surface causes a rapid increase in near-surface sulfate concentration

Supporting Information:

Supporting Information may be found in the online version of this article.

Correspondence to:

T. Liu and X. Huang,
tengyu.liu@nju.edu.cn;
xinhuang@nju.edu.cn

Citation:

Cai, S., Liu, T., Huang, X., Song, Y., Wang, T., Sun, Z., et al. (2024). Important role of low cloud and fog in sulfate aerosol formation during winter haze over the North China Plain. *Geophysical Research Letters*, *51*, e2023GL106597. https://doi.org/10.1029/2023GL106597

Received 30 SEP 2023
Accepted 25 JAN 2024

Abstract Sulfate aerosol greatly contributes to wintertime haze pollution in emission-intensive regions like the North China Plain (NCP) in China. Fast sulfate increase and accumulation are usually recorded during winter haze; however, the multiphase oxidation of sulfur dioxide (SO_2) and the physical processes affecting near-surface sulfate are not fully understood. By combining in situ observations and numerical simulations, we found that high sulfur oxidation ratios (>0.6) under heavily polluted conditions are associated with low clouds and fog over NCP, induced by the moist southerly airflow. Thick low clouds and high SO_2 levels in NCP provide a reaction environment for sulfate production. The sulfate production rate in cloud water can reach 0.5–1.3 μg m^{-3} h^{-1}. The results demonstrate that the vertical mixing of sulfate generated within the cloud water to the surface plays a significant role in rapid sulfate production, highlighting the importance of understanding cloud-water processes in haze pollution.

Plain Language Summary Sulfate has been recognized as an important chemical component of atmospheric aerosols, especially during winter haze events. Rapid increases in sulfate concentrations are frequently observed during heavy pollution in the North China Plain (NCP) of China. However, the processes involved in the multiphase oxidation of sulfur dioxide (SO_2) and the physical processes influencing sulfate variations near the surface remain unclear. In particular, the contribution of traditional in-cloud sulfate production to the surface sulfate has been considered to be negligible in the NCP. Here, we revisited the role of in-cloud sulfate production in the NCP by using ground-based observations, radiosonde measurements, and model simulation. Our results indicate that the rapid conversion of SO_2 to sulfates during heavy pollution is associated with the presence of low clouds and fog. We find that high sulfate production rates in cloud water lead to the rapid accumulation of sulfate, which is vertically mixed to the surface, resulting in a rapid increase in surface sulfate concentrations. This work sheds a new perspective on understanding the role of sulfate production in cloud water and its impact on air pollution.

1. Introduction

Atmospheric sulfate aerosols pose important impacts on air quality, human health, ecosystem, and climate forcing (Carslaw et al., 2010; Charlson et al., 1992; Gurjar et al., 2010; Matsui et al., 2008; Russell & Brunekreef, 2009). Oxidation of sulfur dioxide (SO_2) contributes approximately 80% of the global sulfate (SO_4^{2-}) (Chin et al., 1996; Hung et al., 2018). The traditional sulfate formation mechanisms include the gas-phase oxidation of SO_2 by the hydroxyl radical (OH) and the aqueous-phase oxidation of S(IV) ($=SO_2 \cdot H_2O + HSO_3^- + SO_3^{2-}$) by ozone ($O_3$), hydrogen peroxide ($H_2O_2$), nitrogen dioxide, organic peroxides, and O_2 catalyzed by transition metal ions (TMI) in cloud/fog droplets (Calvert et al., 1978; T. Liu et al., 2021; Pandis & Seinfeld, 2016). In part, it is thought that the most important pathway for sulfate formation in the troposphere is the oxidation of SO_2 by H_2O_2 or O_3 in clouds (Chin et al., 1996; Liang & Jacobson, 1999; Qin et al., 2015; Restad et al., 1998), supported by many aerial surveys and topographic cloud experiments (Benedict et al., 2012; de Valk, 1994; B. Ervens et al., 2018; Harris et al., 2014; Hegg & Hobbs, 1981; Sorooshian et al., 2007; Wonaschuetz et al., 2012). However, many studies proposed that

global/regional atmospheric chemical transport models including traditional sulfate formation mechanisms tend to greatly underestimate sulfate concentrations in highly polluted regions like the North China Plain (NCP), China (Cheng et al., 2016), where mass concentrations of sulfate can reach 20–60 μg m^{-3} and even more than 100 μg m^{-3} during severe winter haze events, accounting for 10%–26% of fine particulate matter ($PM_{2.5}$) (Guo et al., 2014; Han et al., 2016; Y. Liu et al., 2019; Z. Liu et al., 2016; Sun et al., 2016). The dominant sulfate formation pathways in the NCP still remain unclear (Cheng et al., 2016; T. Liu et al., 2021; Tao et al., 2020; Ye et al., 2023; Zheng et al., 2015).

Accordingly, many efforts have been devoted to exploring the previously unappreciated mechanisms of multi-phase oxidation of SO_2 in aerosol particles or at aerosol surfaces (Z. Chen et al., 2022; Cheng et al., 2016; Gen et al., 2019a, 2019; L. Li et al., 2018; T. Liu & Abbatt, 2021; T. Liu et al., 2020; G. Wang et al., 2016; J. Wang et al., 2020; S. Wang et al., 2019; W. Wang et al., 2021; X. Wang et al., 2020; Yao et al., 2019; F. Zhang et al., 2020; L. Zhou et al., 2023). However, the sulfate formation rate in the aerosol water is highly constrained by the liquid water content (LWC) and the pH (Ervens, 2015; Tao et al., 2020). For example, the aerosol LWC under haze conditions in the urban atmosphere varies within hundreds of μg m^{-3}, which is several orders of magnitude lower than ∼0.1 g/m^3 of fog/cloud droplets (Herrmann et al., 2015; T. Liu et al., 2021). Aerosol particles in the NCP are acidic, with pH values ranging from 4 to 5, while fog and cloud droplets are significantly less acidic, with pH ranging from 4.7 to 6.9 (Herrmann et al., 2015; M. Liu et al., 2017; Pye et al., 2020; Song et al., 2018; J. Wang et al., 2020). The above differences in LWC and pH can result in much faster SO_2 oxidation rates and sulfate production rates in clouds than in aerosols in the NCP (Jacobson, 1997; T. Liu et al., 2021). Recent field studies have indicated the potentially important role of in-cloud/fog chemistry in the sulfate aerosol formation in the NCP, though a mechanistic understanding of in-cloud sulfate production is lacking (Sun et al., 2016; J. Wang et al., 2020).

During severe haze conditions, NCP is usually influenced by weak meridional circulation, anomalous southerly and southwesterly winds in the lower troposphere, dominated by the upward movement of warm and humid airflow transmitted from the northwest Pacific Ocean. Water vapor accumulates in front of Taihang Mountain and Yanshan Mountain, prone to form low clouds in the NCP (L. Wang et al., 2014; Wu et al., 2017; R. Zhang et al., 2014; Q. Zhou et al., 2020). However, the numerical representation of low-level cloud or fog is still quite challenging in current weather forecast models (Mueller et al., 2006; Román-Cascón et al., 2012; Sha et al., 2022; Yang et al., 2019), which might hinder our understanding of sulfate formation over this highly polluted region. As many previous studies have focused on the contribution of aerosol chemistry to sulfate production and neglected the impact of traditional cloud/fog chemistry on sulfate, we combine ground-based measurement, radiosonde observations and meteorology-chemistry coupled models to quantitatively understand the mechanisms of sulfate formation in NCP and the contribution from low cloud and fog.

2. Materials and Methods

2.1. WRF-Chem Model Simulation and Processes Analysis

The Weather Research and Forecasting model coupled with Chemistry (WRF-Chem, version 4.1.1) model was used to simulate the sulfate formation (Grell et al., 2005). The domain is centered at 35.0°N, 110.0°E with a grid horizontal resolution of 20 km that covers eastern China and its surrounding areas (Figure S1 in Supporting Information S1). There were 27 vertical levels from the ground level to the top pressure of 50 hPa. The initial meteorological and boundary conditions were obtained from the fifth-generation ECMWF reanalysis for the global climate and weather (ERA5). Anthropogenic emission data were obtained from the Multi-resolution Emission Inventory for China (MEIC) model. Recent studies using top-down inversion models and satellite retrievals found that the MEIC inventory overpredicted SO_2 emissions by 1–2 times (D. Chen et al., 2016; N. Li et al., 2021; Sha et al., 2019). Accordingly, SO_2 emissions were reduced by half to better match observations. As shown in Figure S2 in Supporting Information S1, the simulated SO_2 concentrations were more consistent with the observations after the modification of SO_2 emissions. The CBMZ (Carbon Bond Mechanism) photochemical mechanism and MADE/SORGAM (Modal Aerosol Dynamics Model for Europe with the Secondary Organic Aerosol Model) aerosol model and the improved ISORROPIA II model were used in this study (Ackermann et al., 1998; Fast et al., 2006; Fountoukis & Nenes, 2007; Nenes et al., 1998; Schell et al., 2001). The improved ISORROPIA-II model was used to simulate aerosol dynamics including nucleation, coagulation, condensation and their thermodynamic equilibrium, providing the pH, aerosol water content

(AWC) and concentrations of species in the gas, liquid, as well as solid phases at chemical equilibrium (Fountoukis & Nenes, 2007; Nenes et al., 1998). We have improved the aqueous phase chemistry in the aerosol model based on previous studies (T. Wang et al., 2022; W. Wang et al., 2021), including additional sulfate formation pathways on/in the aerosol particles and the reaction of HCHO and S(IV) to form hydroxymethanesulfonate. Details of the model modifications are described in Text S2 in Supporting Information S1. The main configuration options and domain settings for the model are listed in Table S1 and Figure S1 in Supporting Information S1. The main sulfate formation pathways in cloud water of WRF-Chem are given in Table S3 in Supporting Information S1.

Diagnostic analysis tools in WRF-Chem modeling, which include vertical mixing (vmix), gas-phase and cloud-phase chemistry (chem), and advection (adv), were used to investigate the contributions of physical and chemical processes to variations in SO_4^{2-} concentrations. Detailed information on model simulation and process analysis is provided in Text S3 in Supporting Information S1.

2.2. Observational Data Set

To evaluate the model performance, surface meteorological data were collected from seven stations, where Beijing, Tangshan, Tianjin, Jinan, and Zhengzhou are located in the NCP, and Shanghai and Nanjing are located in the Yangtze River Delta. The locations of the above stations are shown in Figure S1 in Supporting Information S1. The meteorological variables included hourly temperature at 2 m (T2), relative humidity at 2 m (RH2), and wind speed at 10 m (WS10) were available with observational data from automatic meteorological station archived in NOAA National Climatic Data Center (NCDC). The statistics included correlation coefficient (R), mean bias (MB), root mean square error (RMSE), and normalized mean bias (NMB). The simulated pollutants were evaluated using hourly observations of $PM_{2.5}$, SO_2 and NO_2 from the above seven ground-based monitoring stations. Water soluble aerosol ions (i.e., NO_3^-, SO_4^{2-}, NH_4^+, Na^+, K^+, Cl^-, Ca^{2+}, Mg^{2+}, etc.) were measured by a Monitor for Aerosols and Gases in ambient Air (MARGA) in Beijing with a time resolution of 1 hourly.

Following the dewpoint depression (ΔT_d) threshold method (Poore et al., 1995), radiosonde data at Beijing were used to identify the cloud base height of the low cloud. The meteorological data are from ERA5 with a temporal resolution of 1 hr, a horizontal resolution of 0.25° × 0.25° and a vertical resolution of 37 pressure levels ranging from 1,000 hPa to 1 hPa.

2.3. Dewpoint Depression Threshold Method

The dewpoint depression (ΔT_d) threshold method was adopted to identify the presence of clouds during sounding periods, and the cloud layer was confirmed when the dewpoint depression was below the set threshold (Poore et al., 1995). The reference threshold was set as:

$$\Delta T_d = \begin{cases} 1.7℃ & (T > 0℃) \\ 3.4℃ & (-20℃ \le T \le 0℃) \\ 5.2℃ & (T < -20℃)) \end{cases}$$

By judging the relationship between ΔT_d and threshold at each height, the cloud base height can be identified.

3. Results and Discussions

3.1. Low Clouds in the NCP and the Linkage With Sulfate Formation

Figure 1a shows that high concentrations of $PM_{2.5}$ frequently shroud Beijing and its surrounding areas during cold winters, and the average $PM_{2.5}$ concentration can reach more than 60 μg/m^3 in winter 2013–2017. Sulfate mass concentration can account for 6%–12% of $PM_{2.5}$ (Figure 1a). The number of samples for $PM_{2.5}$ from ground-based monitoring stations, SO_4^{2-}, NO_3^-, and NH_4^+ from MARGA were 8872, 6844, 6814, and 6780, respectively. To identify the atmospheric humidity and low clouds (cloud base height <2 km) and their association with sulfate formation in the NCP, we conducted a statistical analysis of Beijing in winter from 2013 to 2017. Sounding data statistics show that low clouds are common in winter

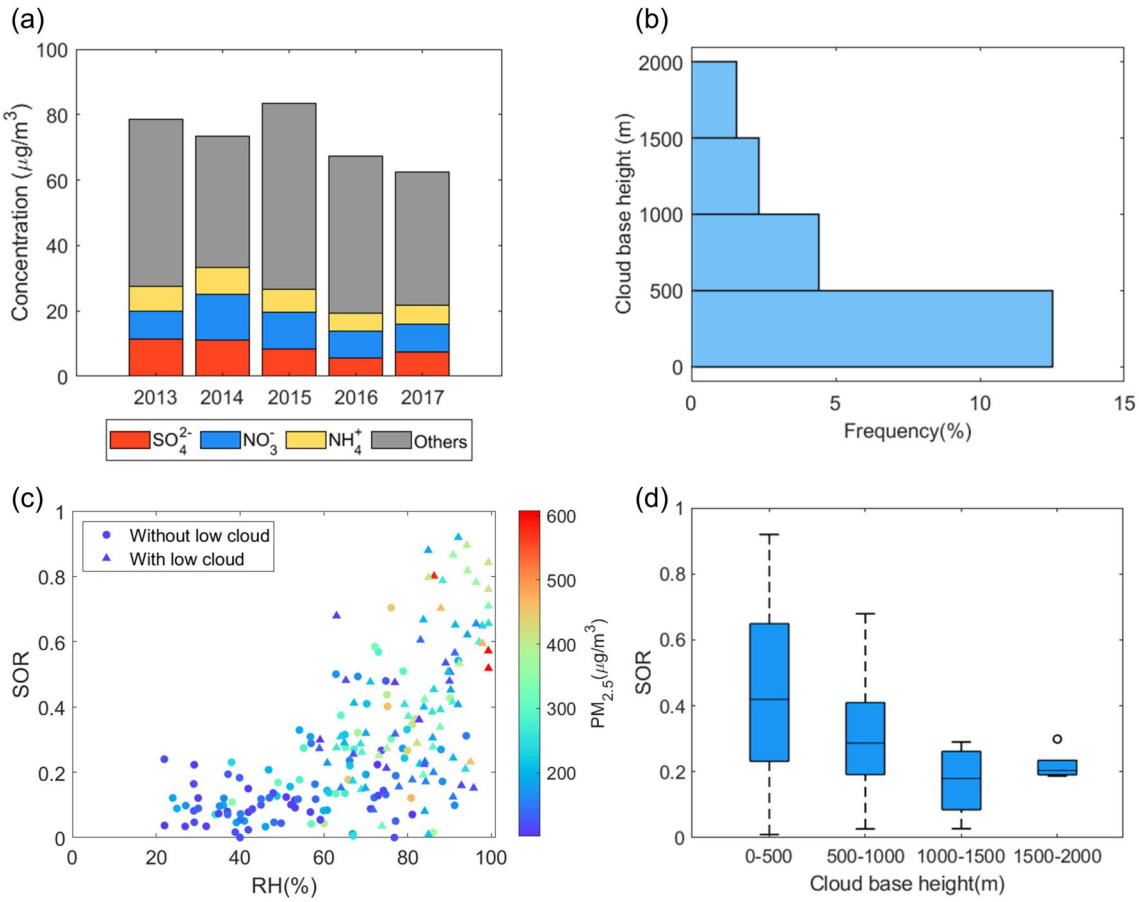

Figure 1. Wintertime aerosol pollution and low clouds in Beijing during 2013–2017. (a) Chemical compositions of $PM_{2.5}$ observed in Beijing from 2013 to 2017 in winter. (b) A histogram showing cloud base height of low cloud calculated by atmospheric sounding at 8:00 and 20:00 LT (local time). (c) Scatter plot of sulfur oxidation ratio (SOR) versus relative humidity (RH) with low cloud (triangle) and without low cloud (dots) at 8:00 and 20:00 LT with $PM_{2.5}$ greater than 100 μg/m^3. The filling color indicates the concentration of $PM_{2.5}$. (d) Distribution of SOR at different cloud base heights.

over the NCP. In Beijing, for instance, the frequency of low clouds in winter is 20.8% of the whole season, among which the probability of low clouds with the cloud base height (CBH) below 500 m is the highest at 12.5%, accounting for half of the total low cloud frequency (Figure 1b). Due to the low SO_2 concentration and high CBH in the medium and high clouds, as well as the middle and uppermost layers of the multilayer clouds (Q. Zhou et al., 2020), the transport of sulfate aerosol to the surface becomes difficult, so this study focuses on the impact of low clouds on sulfate aerosol formation. The sulfate oxidation ratio (SOR, molar ratio of sulfate to the sum of sulfate and SO_2), which has been extensively used to indicate the conversion efficiency of sulfur in the atmosphere (P. Liu et al., 2020; X. Wang et al., 2019; R. Zhang et al., 2018), increased with increasing relative humidity (RH) for conditions both with and without low clouds when pollution occurs ($PM_{2.5}$ concentration greater than 100 μg/m^3) in Beijing. SOR sharply increases at RH greater than 60%, highlighting the importance of aqueous-phase sulfate formation. In the case of high RH, the SOR is significantly higher in the presence of low clouds than in the absence of low clouds, which suggests that the sulfate conversion efficiency is higher in clouds than that in aerosol water. A significant fraction of the data with low clouds at RH in the range of 80%–100% is associated with SOR above 0.6 and most of them correspond to heavy pollution events with $PM_{2.5}$ above 400 μg/m^3. This suggests that heavy pollution with larger SOR is often accompanied by high RH with low clouds.

The surface SOR for CBH below 500 m is widely distributed in 0.2–0.7 and can reach up to 0.95 or higher (Figure 1d). With the increase of height, the frequency of low clouds at the corresponding height gradually declines, so does the surface SOR. SOR is mainly below 0.3 for CBH of 1,000–2,000 m with a frequency of less than 5%, which indicates that low cloud with lower CBH is more likely to impact the formation of sulfate aerosols.

3.2. Vertical Insights Into Different Oxidation Pathways of SO_2

To further explore the weather conditions for low cloud and its role in sulfate formation under heavily polluted conditions in the NCP, we performed a WRF-Chem model analysis for a severe haze-cloud event for a consecutive week from 6 to 15 December 2015. A haze event accompanied by low cloud and fog formation was observed in the NCP. In this case, we found fast sulfate formation accompanied by high RH near the surface and low clouds in Beijing. Figure 2a shows the observed time series of hourly temperature, RH, $PM_{2.5}$ and sulfate concentrations in Beijing. From 6 to 10 December, $PM_{2.5}$ concentrations gradually increased and exceeded 350 μg/m^3 on 10 December, leading to severe air pollution. From noon on 7 December, the sulfate concentration increased rapidly and reached 30 μg/m^3 within a short period of time, which is highly consistent with the observed low cloud period. It is worth noting that the absence of bars could also be caused by the missing data of CBH.

The performance statistics for the meteorological prediction of WRF-Chem are shown in Table S4 in Supporting Information S1. The predicted meteorological variables matched well with the observations, such as T2, RH2, and WS10, with correlation coefficients of 0.92, 0.86, and 0.63, respectively. The MB, RMSE, and NMB of hourly T2, RH2, and WS10 were also small. The model reasonably reproduced the temporal variations and magnitudes of the meteorological variables, confirming the credibility of the meteorological simulations. The model simulation has also been validated by available air pollutant observations (Figures S3 and S4 in Supporting Information S1). Due to uncertainties in emission inventories, meteorological fields and chemical mechanisms, the liquid water content in low clouds/fog was not simulated accurately, resulting in an underestimation of $PM_{2.5}$ in Shanxi and Shaanxi. But considering that this study focuses on exploring the variation of sulfate during this haze-cloud event in the NCP, the good agreement between the simulated and observed $PM_{2.5}$ in most areas of the NCP indicates that the simulation is able to capture this pollution event (Figures 2b and 2c). Combining the evolution of the weather situation with the simulated $PM_{2.5}$, it was found that the anticyclone was located along the Yellow Sea on 8 December (Figure 2e). Beijing was located at the northwestern edge of the anticyclone, with prevailing southerly upward winds at 925 hPa (Figure S5 in Supporting Information S1). Accompanied by warm and moist airflow delivered from the northwestern Pacific Ocean, the atmospheric humidity in Beijing would increase. The statistics revealed that the southerly or southwesterly wind accounted for more than half of the low cloud periods in Beijing during winter (Figure S6 in Supporting Information S1). This large-scale meteorological field led to upward airflow and water vapor transport, which contributed to the formation of clouds and fog. Also, the topography of Taihang Mountain and Yanshan Mountain (marked in Figure S1 in Supporting Information S1) facilitated uplift and prevented water vapor diffusion, low clouds and fog were maintained, thus providing sufficient liquid water for aqueous-phase chemistry. The RH below 1.5 km altitude in Beijing was maintained at high levels of 80%–100%, in which sulfate accumulated rapidly (Figures 2a and 2d). Under the effect of high-pressure western airflow, $PM_{2.5}$ was rapidly generated and reached 200 μg/m^3 in the area of central and northern China. On 9 December, the offshore anticyclone moved eastward and weakened (Figure 2f). The pressure gradient on the ground in Beijing was smaller and the wind speed was weaker, which was not conducive to the diffusion of pollutants. Moreover, due to the influence of topography, pollutants accumulated and gathered faster in front of the mountains, forming a southwest-northeast pollution belt along the side of Taihang Mountain and Yanshan Mountain, thus blocking further west-northward transport of pollutants.

During this haze pollution case, sulfate showed a rapid increase from 10 to 45 μg/m^3 on 8 December, and the vertical distribution of both aerosol and cloud featured great heterogeneity. To quantitatively understand the sulfate production in different vertical layers during this pollution event, we diagnosed the reaction rate of various chemical pathways in WRF-Chem model, including sulfate production pathways in the gas phase, in cloud water and in aerosol water, namely oxidation by dissolved O_3, H_2O_2, NO_2, and TMI (in the presence of O_2), and its contributions to the vertical sulfate production over the NCP (shown in the rectangle of Figure 4b) during the high sulfate period in Figure 3. Below 1.2 km altitude, the sulfate formation rate was highly dependent on the sulfate oxidation in cloud or fog water, which means that sulfate formation rates in cloud or fog water accounted for more than 80% of the total rate (Figure 3a). For the 200–400 m altitude (blue rectangular area), the higher cloud water content led to a maximum of 0.5–1.3 μg m^{-3} h^{-1} in-cloud sulfate formation rate. The gas-phase oxidation rate and the aqueous-phase oxidation rate in aerosol water were on the order of 10^{-3} and 10^{-2} μg m^{-3} h^{-1}, respectively, which were negligible compared to that of in-cloud sulfate formation rate.

The average rates of four sulfate formation pathways in cloud water were non-uniform vertically (Figure 3b). The sulfate production rate in fog, namely the lowest layer of cloud in the model, could reach 0.3 μg m^{-3} h^{-1}. To

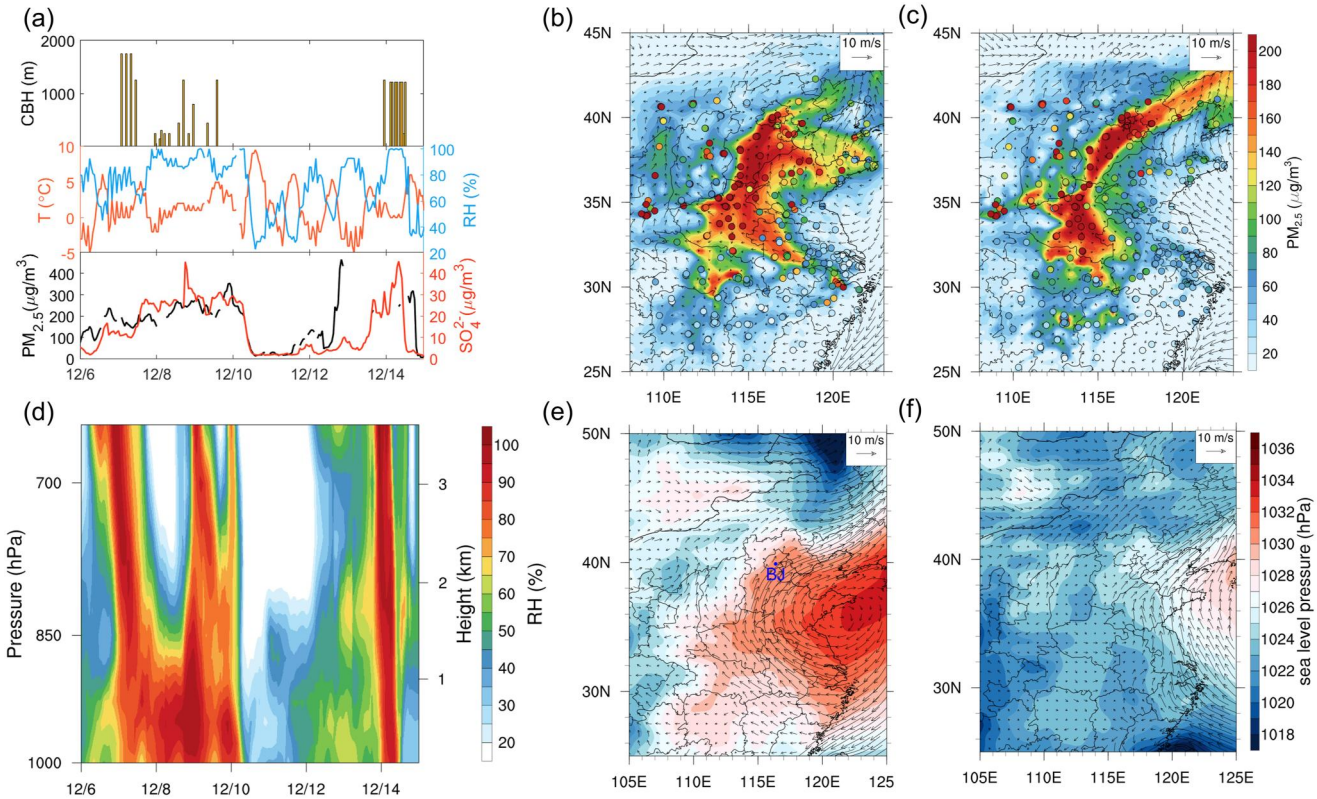

Figure 2. Typical haze event in the NCP from 6–15 December 2015. (a) Time series of meteorological parameters (cloud base height (CBH) air temperature (T), RH) obtained from NCDC, the concentrations of $PM_{2.5}$ and sulfate observed in Beijing. WRF-Chem simulated surface $PM_{2.5}$ mass concentrations and wind field at (b) 12:00 LT on 8 December and (c) 12:00 LT on 9 December. Color dots represent observed $PM_{2.5}$ mass concentrations. (d) Vertical distribution of RH from ERA5 in Beijing. Spatial distributions of sea level pressure and 925-hPa wind field from ERA5 at (e) 12:00 LT on 8 December, (f) 12:00 LT on 9 December.

illustrate the role of sulfate production in fog, we added an experiment with the fog chemistry turned off. Compared to the fog-off experiment, the impact of turning on fog chemistry on sulfate was relatively small, with surface sulfate changing by only less than 5% in the high-sulfate region (Figure S7 in Supporting Information S1). With the higher pH of 5–7 in cloud water (Figure S8 in Supporting Information S1), both O_3 and NO_2 oxidation pathways played the dominant role below 1 km. The contribution of the TMI pathway was relatively small, while that of the H_2O_2 pathway was negligible. The vertical variation of the above pathways could be caused by the differences in the vertical distribution of cloud water content, precursor concentrations, pH in cloud water, oxidant concentration, and catalyst concentration (T. Liu et al., 2021; Pandis & Seinfeld, 2016). As the low cloud was distributed at a low altitude in this case, reaction rates decreased due to the decreasing cloud water content with increasing altitude above 300 m. Aqueous phase sulfate production in cloud water became negligible at altitudes higher than 1 km.

3.3. Accelerated Sulfate Formation by Low Cloud and Its Impact on $PM_{2.5}$ Pollution

To quantitatively elucidate the contributions of different physical or chemical processes to surface sulfate, we analyzed the simulated concentrations of sulfate aerosols using the WRF-Chem diagnostic analysis technique mentioned in Text S3 in Supporting Information S1. Figure 4a shows the contributions of chemical processes, vertical mixing process with dry deposition and advection transport processes to the sulfate at the surface of Beijing. The simulation results showed that the vertical mixing process had the largest absolute average contribution of 61% and posed a very high positive contribution during the daytime on both 8 and 9 December. In other words, the vertical distribution of sulfate aerosol was highly stratificated.

Though the concentration of the gas precursor SO_2 near the surface was over 2–5 times higher than at the altitude of 300 m, as aforementioned, the sulfate production rate was higher in the upper air. Based on the model diagnosis, sulfate chemical formation at 300 m, exceeded 20 μg m^{-3} h^{-1}, which was 20 times higher than the near-

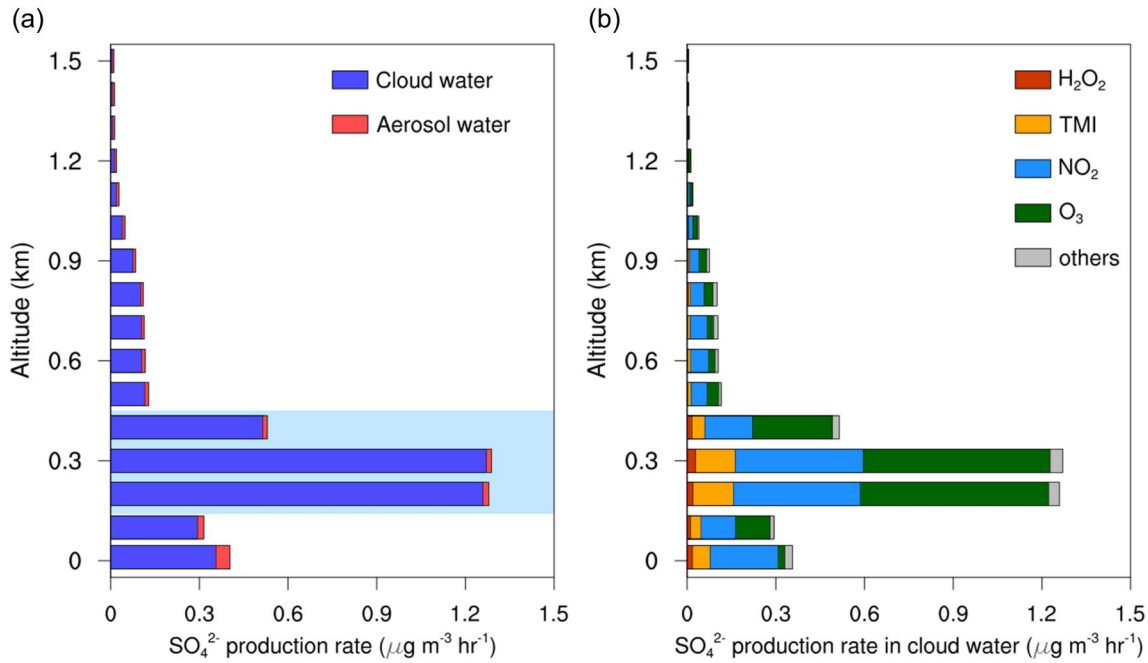

Figure 3. Vertical distribution of different pathways for sulfate production. Contribution of averaged sulfate production rate over the rectangle area marked in Figure 4b with white solid line (a) in aerosol water and cloud water, as well as (b) different reaction pathways with O_3, H_2O_2, NO_2, TMI-catalyzed and others in cloud water are shown in bar charts from 00:00 LT 8 December 2015 to 00:00 LT 10 December 2015. Cloudy height ranges are shown in (a) with a light blue rectangle.

surface rate of 1 μg m^{-3} h^{-1} during the same time period. The fastly formed sulfate was then entrained downward by convective mixing (Figure S9 in Supporting Information S1), significantly enhancing the near-surface sulfate aerosol concentrations, and the above results can be generalized to the NCP (Figure S10 in Supporting Information S1). Moreover, the boundary layer started to develop in the morning, at which time convective mixing was most prominent, near-surface sulfate concentration rose by 40 μg m^{-3} in less than 4 hr during the daytime on December 8. Therefore, we further analyzed the diagnostic results of the vertical profile of sulfate from 10:00 to 13:00 LT on December 8.

Surface sulfate aerosols from 10:00 to 13:00 LT on December 8 were mainly concentrated in the northern part of the NCP and were highly coincident with the regions where low clouds existed (average cloud water content higher than 0.1 g/m^3) below 2 km (Figure 4b). The overall high value of sulfate was mostly distributed below 600 m (Figure 4c). The height range between 200 and 400 m was the region where the high value of sulfate chemical formation in cloud water (Figure 4d). More than 30 μg/m^3 of sulfate was rapidly generated within 4 hr where the low cloud was concentrated. Such a fast chemical production of sulfate in the aqueous phase of cloud water and vigorous vertical mixing during the daytime would substantially raise the sulfate concentration near the surface, thereby further deteriorating $PM_{2.5}$ pollution.

4. Atmospheric Implications

In this study, the role of aqueous-phase sulfate chemistry in clouds during a heavy haze event over NCP in 2015 was investigated by combining ground-based observations, radiosonde measurements together with model simulation. We found that during the pre-pollution period, Beijing was influenced by a high-pressure system with prevailing southerly winds at 925 hPa, and the updrafts were accompanied by warm and humid airflow delivered from the northwest Pacific Ocean, which facilitated the formation of low clouds and fog. Low clouds enabled a sufficiently high sulfate production rate of up to 0.5–1.3 μg m^{-3} h^{-1}, overwhelmingly exceeding the sulfate formation rate in the gas phase and in aerosol water. The sulfate produced within the clouds was deposited to the surface via vertical mixing, together with sulfate produced in the fog at the surface, which exerted an important impact on the rapid sulfate production and haze formation in winter over the NCP. Our results show that the frequency of such low cloud events in winter in NCP is 20.8%, highlighting the important role of in-cloud sulfate

10.1029/2023GL106597

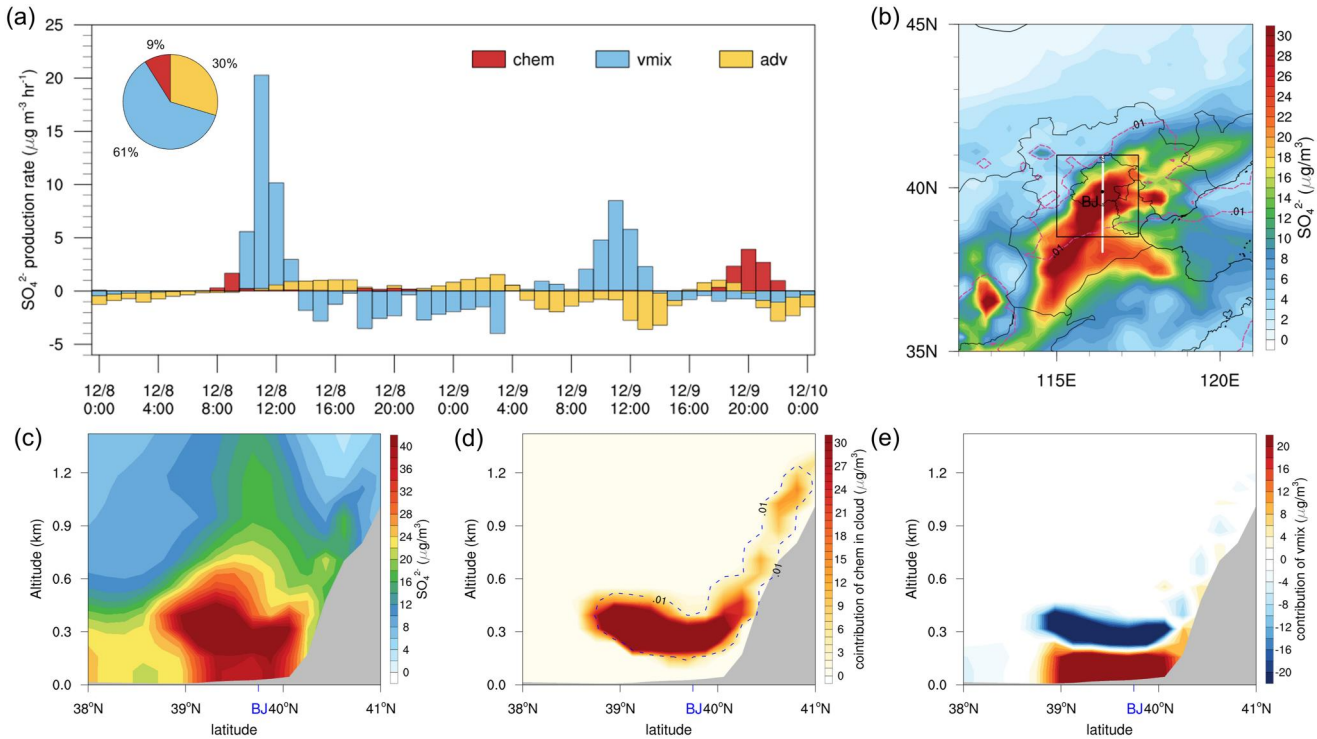

Figure 4. WRF-Chem simulated sulfate concentrations and contributions of different processes to sulfate at the time with low cloud. (a) Time series of SO_4^{2-} production rate of physical/chemical processes (vmix = vertical mixing with dry deposition; chem = chemical production; adv = horizontal and vertical advection) at the surface in Beijing (BJ, marked in (b)) from 00:00 LT 8 December 2015 to 00:00 LT 10 December 2015. The pie chart shows fractional contributions of absolute production rate over the above time period. (b) WRF-Chem simulated averaged sulfate concentrations at the surface from 10:00 LT December 2015 to 13:00 LT 8 December 2015, together with averaged cloud water content under 2 km, which is greater than 0.01 g/m^3 (pink dash line). Simulated vertical cross section of (c) averaged SO_4^{2-} concentrations, (d) accumulated contribution of chem on SO_4^{2-} in cloud, together with averaged cloud water content greater than 0.01 g/m^3 (blue dash line), and (e) accumulated contribution of vmix on SO_4^{2-} during 10:00 LT 8 December 2015 to 13:00 LT 8 December 2015 along the white solid line marked in (b) at longitude of 116.32°E (BJ indicates the location of BJ). The gray shadows indicated the terrain.

production. For cloud-free conditions, multiphase sulfate chemistry in aerosol water may become the dominant sulfate production pathway.

Our study demonstrates that the in-cloud sulfate formation has an important impact on winter sulfate aerosol in highly polluted environments. In particular, the accurate simulation of low clouds affects the vertical and spatial distribution of sulfate aerosols. There is a need for an improved understanding of the role of in-cloud chemistry in haze pollution. Furthermore, such low cloud chemistry may play an important role in sulfate aerosol formation in remote environments, such as the Tibetan Plateau where low clouds prevail (Duan & Wu, 2006). As well, the sulfate aerosol would interplay with the weather and climate in this region (Zhao et al., 2019).

Conflict of Interest

The authors declare no conflicts of interest relevant to this study.

Data Availability Statement

Anthropogenic emission data obtained from Multi-resolution Emission Inventory for China (http://meicmodel.org.cn/?page_id=541&lang=en). ERA5 meteorological parameters on pressure levels are available at Hersbach et al. (2023a) and meteorological parameters on single levels are obtained from Hersbach et al. (2023b). The surface meteorological data are available at https://www.ncei.noaa.gov/access/search/data-search/global-hourly. The ambient air monitoring data, including $PM_{2.5}$, SO_2, and NO_2 are archived at a repository of Chinese National Environmental Monitoring Center (http://www.cnemc.cn/sssj/). Sounding data can be found at the University of

Wyoming (http://weather.uwyo.edu/upperair/sounding.html). Main surface observation data is archived on the website of Figshare (Cai et al., 2024). Figures in this article are processed with the NCAR Command Language version 6.6.2 (NCAR, 2019) and the software MATLAB Release 2021a (MathWorks, 2021).

Acknowledgments
The authors thank the National Natural Science Foundation of China projects (92044301, 42222504, 42175112), the Second Tibetan Plateau Scientific Expedition and Research (STEP) program (2019QZKK0106), the Fundamental Research Funds for the Central Universities (14380187), and Natural Science Foundation of Jiangsu Province (BK20210195) for funding. T. Liu thanks the Jiangsu Provincial "Double Innovation Doctorate" program (JSSCBS20210025) for funding.

References

Ackermann, I. J., Hass, H., Memmesheimer, M., Ebel, A., Binkowski, F. S., & Shankar, U. (1998). Modal aerosol dynamics model for Europe: Development and first applications. *Atmospheric Environment*, *32*(17), 2981–2999. https://doi.org/10.1016/S1352-2310(98)00006-5

Benedict, K. B., Lee, T., & Collett, J. L. (2012). Cloud water composition over the southeastern Pacific Ocean during the VOCALS regional experiment. *Atmospheric Environment*, *46*, 104–114. https://doi.org/10.1016/j.atmosenv.2011.10.029

Cai, S., Liu, T., & Huang, X. (2024). BJ_MARGA_Surfacedata.xlsx [Dataset]. Figshare. https://doi.org/10.6084/m9.figshare.24958776

Calvert, J. G., Bottenheim, J. W., & Strausz, O. P. (1978). Mechanism of the homogeneous oxidation of sulfur dioxide in the troposphere. In R. B. Husar, J. P. Lodge, & D. J. Moore (Eds.), *Sulfur in the atmosphere* (pp. 197–226). Pergamon.

Carslaw, K. S., Boucher, O., Spracklen, D. V., Mann, G. W., Rae, J. G. L., Woodward, S., & Kulmala, M. (2010). A review of natural aerosol interactions and feedbacks within the Earth system. *Atmospheric Chemistry and Physics*, *10*(4), 1701–1737. https://doi.org/10.5194/acp-10-1701-2010

Charlson, R. J., Schwartz, S. E., Hales, J. M., Cess, R. D., Coakley, J. A., Hansen, J. E., & Hofmann, D. J. (1992). Climate forcing by anthropogenic aerosols. *Science*, *255*(5043), 423–430. https://doi.org/10.1126/science.255.5043.423

Chen, D., Liu, Z., Fast, J., & Ban, J. (2016). Simulations of sulfate–nitrate–ammonium (SNA) aerosols during the extreme haze events over northern China in October 2014. *Atmospheric Chemistry and Physics*, *16*(16), 10707–10724. https://doi.org/10.5194/acp-16-10707-2016

Chen, Z., Liu, P., Wang, W., Cao, X., Liu, Y.-X., Zhang, Y.-H., & Ge, M. (2022). Rapid sulfate formation via uncatalyzed autoxidation of sulfur dioxide in aerosol microdroplets. *Environmental Science & Technology*, *56*(12), 7637–7646. https://doi.org/10.1021/acs.est.2c00112

Cheng, Y., Zheng, G., Wei, C., Mu, Q., Zheng, B., Wang, Z., et al. (2016). Reactive nitrogen chemistry in aerosol water as a source of sulfate during haze events in China. *Science Advances*, *2*(12), e1601530. https://doi.org/10.1126/sciadv.1601530

Chin, M., Jacob, D. J., Gardner, G. M., Foreman-Fowler, M. S., Spiro, P. A., & Savoie, D. L. (1996). A global three-dimensional model of tropospheric sulfate. *Journal of Geophysical Research*, *101*(13), 18667–18690. https://doi.org/10.1029/96jd01221

de Valk, J. P. J. M. M. (1994). A model for cloud chemistry: A comparison between model simulations and observations in stratus and cumulus. *Atmospheric Environment*, *28*(9), 1665–1678. https://doi.org/10.1016/1352-2310(94)90312-3

Duan, A., & Wu, G. (2006). Change of cloud amount and the climate warming on the Tibetan Plateau. *Geophysical Research Letters*, *33*(22). https://doi.org/10.1029/2006GL027946

Ervens, B. (2015). Modeling the processing of aerosol and trace gases in clouds and fogs. *Chemical Reviews*, *115*(10), 4157–4198. https://doi.org/10.1021/cr5005887

Ervens, B., Sorooshian, A., Aldhaif, A. M., Shingler, T., Crosbie, E., Ziemba, L., et al. (2018). Is there an aerosol signature of chemical cloud processing? *Atmospheric Chemistry and Physics*, *18*(21), 16099–16119. https://doi.org/10.5194/acp-18-16099-2018

Fast, J. D., Gustafson, W. I., Jr., Easter, R. C., Zaveri, R. A., Barnard, J. C., Chapman, E. G., et al. (2006). Evolution of ozone, particulates, and aerosol direct radiative forcing in the vicinity of Houston using a fully coupled meteorology-chemistry-aerosol model. *Journal of Geophysical Research*, *111*(D21). https://doi.org/10.1029/2005JD006721

Fountoukis, C., & Nenes, A. (2007). ISORROPIA II: A computationally efficient thermodynamic equilibrium model for K^+–Ca^{2+}–Mg^{2+}–NH_4^+–Na^+–SO_4^{2-}–NO_3^-–Cl^-–H_2O aerosols. *Atmospheric Chemistry and Physics*, *7*(17), 4639–4659. https://doi.org/10.5194/acp-7-4639-2007

Gen, M., Zhang, R., Huang, D. D., Li, Y., & Chan, C. K. (2019a). Heterogeneous SO_2 oxidation in sulfate formation by photolysis of particulate nitrate. *Environmental Science and Technology Letters*, *6*(2), 86–91. https://doi.org/10.1021/acs.estlett.8b00681

Gen, M., Zhang, R., Huang, D. D., Li, Y., & Chan, C. K. (2019b). Heterogeneous oxidation of SO_2 in sulfate production during nitrate photolysis at 300 nm: Effect of pH, relative humidity, irradiation intensity, and the presence of organic compounds. *Environmental Science & Technology*, *53*(15), 8757–8766. https://doi.org/10.1021/acs.est.9b01623

Grell, G. A., Peckham, S. E., Schmitz, R., McKeen, S. A., Frost, G., Skamarock, W. C., & Eder, B. (2005). Fully coupled "online" chemistry within the WRF model. *Atmospheric Environment*, *39*(37), 6957–6975. https://doi.org/10.1016/j.atmosenv.2005.04.027

Guo, S., Hu, M., Zamora, M. L., Peng, J., Shang, D., Zheng, J., et al. (2014). Elucidating severe urban haze formation in China. *Proceedings of the National Academy of Sciences of the United States of America*, *111*(49), 17373–17378. https://doi.org/10.1073/pnas.1419604111

Gurjar, B. R., Jain, A., Sharma, A., Agarwal, A., Gupta, P., Nagpure, A. S., & Lelieveld, J. (2010). Human health risks in megacities due to air pollution. *Atmospheric Environment*, *44*(36), 4606–4613. https://doi.org/10.1016/j.atmosenv.2010.08.011

Han, B., Zhang, R., Yang, W., Bai, Z., Ma, Z., & Zhang, W. (2016). Heavy haze episodes in Beijing during January 2013: Inorganic ion chemistry and source analysis using highly time-resolved measurements from an urban site. *Science of the Total Environment*, *544*, 319–329. https://doi.org/10.1016/j.scitotenv.2015.10.053

Harris, E., Sinha, B., van Pinxteren, D., Schneider, J., Poulain, L., Collett, J., et al. (2014). In-cloud sulfate addition to single particles resolved with sulfur isotope analysis during HCCT-2010. *Atmospheric Chemistry and Physics*, *14*(8), 4219–4235. https://doi.org/10.5194/acp-14-4219-2014

Hegg, D. A., & Hobbs, P. V. (1981). Cloud water chemistry and the production of sulfates in clouds. *Atmospheric Environment*, *15*(9), 1597–1604. https://doi.org/10.1016/0004-6981(81)90144-X

Herrmann, H., Schaefer, T., Tilgner, A., Styler, S. A., Weller, C., Teich, M., & Otto, T. (2015). Tropospheric aqueous-phase chemistry: Kinetics, mechanisms, and its coupling to a changing gas phase. *Chemical Reviews*, *115*(10), 4259–4334. https://doi.org/10.1021/cr500447k

Hersbach, H., Bell, B., Berrisford, P., Biavati, G., Horányi, A., Muñoz Sabater, J., et al. (2023a). ERA5 hourly data on pressure levels from 1940 to present [Dataset]. Copernicus Climate Change Service (C3S) Climate Data Store (CDS). https://doi.org/10.24381/cds.bd0915c6

Hersbach, H., Bell, B., Berrisford, P., Biavati, G., Horányi, A., Muñoz Sabater, J., et al. (2023b). ERA5 hourly data on single levels from 1940 to present [Dataset]. Copernicus Climate Change Service (C3S) Climate Data Store (CDS). https://doi.org/10.24381/cds.adbb2d47

Hung, H.-M., Hsu, M.-N., & Hoffmann, M. R. (2018). Quantification of SO_2 oxidation on interfacial surfaces of acidic micro-droplets: Implication for ambient sulfate formation. *Environmental Science & Technology*, *52*(16), 9079–9086. https://doi.org/10.1021/acs.est.8b01391

Jacobson, M. Z. (1997). Development and application of a new air pollution modeling system—II. Aerosol module structure and design. *Atmospheric Environment*, *31*(2), 131–144. https://doi.org/10.1016/1352-2310(96)00202-6

Li, L., Hoffmann, M. R., & Colussi, A. J. (2018). Role of nitrogen dioxide in the production of sulfate during Chinese haze-aerosol episodes. *Environmental Science & Technology*, *52*(5), 2686–2693. https://doi.org/10.1021/acs.est.7b05222

Li, N., Tang, K., Wang, Y., Wang, J., Feng, W., Zhang, H., et al. (2021). Is the efficacy of satellite-based inversion of SO_2 emission model dependent? *Environmental Research Letters*, *16*(3), 035018. https://doi.org/10.1088/1748-9326/abe829

Liang, J., & Jacobson, M. Z. (1999). A study of sulfur dioxide oxidation pathways over a range of liquid water contents, pH values, and temperatures. *Journal of Geophysical Research*, *104*(D11), 13749–13769. https://doi.org/10.1029/1999JD900097

Liu, M., Song, Y., Zhou, T., Xu, Z., Yan, C., Zheng, M., et al. (2017). Fine particle pH during severe haze episodes in northern China. *Geophysical Research Letters*, *44*(10), 5213–5221. https://doi.org/10.1002/2017GL073210

Liu, P., Ye, C., Xue, C., Zhang, C., Mu, Y., & Sun, X. (2020). Formation mechanisms of atmospheric nitrate and sulfate during the winter haze pollution periods in Beijing: Gas-phase, heterogeneous and aqueous-phase chemistry. *Atmospheric Chemistry and Physics*, *20*(7), 4153–4165. https://doi.org/10.5194/acp-20-4153-2020

Liu, T., & Abbatt, J. P. D. (2021). Oxidation of sulfur dioxide by nitrogen dioxide accelerated at the interface of deliquesced aerosol particles. *Nature Chemistry*, *13*(12), 1173–1177. https://doi.org/10.1038/s41557-021-00777-0

Liu, T., Chan, A. W. H., & Abbatt, J. P. D. (2021). Multiphase oxidation of sulfur dioxide in aerosol particles: Implications for sulfate formation in polluted environments. *Environmental Science & Technology*, *55*(8), 4227–4242. https://doi.org/10.1021/acs.est.0c06496

Liu, T., Clegg, S. L., & Abbatt, J. P. D. (2020). Fast oxidation of sulfur dioxide by hydrogen peroxide in deliquesced aerosol particles. *Proceedings of the National Academy of Sciences of the United States of America*, *117*(3), 1354–1359. https://doi.org/10.1073/pnas.1916401117

Liu, Y., Zheng, M., Yu, M., Cai, X., Du, H., Li, J., et al. (2019). High-time-resolution source apportionment of $PM_{2.5}$ in Beijing with multiple models. *Atmospheric Chemistry and Physics*, *19*(9), 6595–6609. https://doi.org/10.5194/acp-19-6595-2019

Liu, Z., Hu, B., Zhang, J., Yu, Y., & Wang, Y. (2016). Characteristics of aerosol size distributions and chemical compositions during wintertime pollution episodes in Beijing. *Atmospheric Research*, *168*, 1–12. https://doi.org/10.1016/j.atmosres.2015.08.013

MATLAB version: 9.10.0 (R2021a). (2021). MATLAB version: 9.10.0 (R2021a) [Software]. The MathWorks Inc. Retrieved from https://www.mathworks.com

Matsui, T., Beltrán-Przekurat, A., Niyogi, D., Pielke, R. A., Sr., & Coughenour, M. (2008). Aerosol light scattering effect on terrestrial plant productivity and energy fluxes over the eastern United States. *Journal of Geophysical Research*, *113*(D14). https://doi.org/10.1029/2007JD009658

Mueller, S. F., Bailey, E. M., Cook, T. M., & Mao, Q. (2006). Treatment of clouds and the associated response of atmospheric sulfur in the community multiscale air quality (CMAQ) modeling system. *Atmospheric Environment*, *40*(35), 6804–6820. https://doi.org/10.1016/j.atmosenv.2006.05.069

Nenes, A., Pandis, S. N., & Pilinis, C. (1998). ISORROPIA: A new thermodynamic equilibrium model for multiphase multicomponent inorganic aerosols. *Aquatic Geochemistry*, *4*(1), 123–152. https://doi.org/10.1023/A:1009604003981

Pandis, S. N., & Seinfeld, J. H. (2016). *Atmospheric chemistry and physics: From air pollution to climate change*. Wiley.

Poore, K. D., Wang, J., & Rossow, W. B. (1995). Cloud layer thicknesses from a combination of surface and upper-air observations. *Journal of Climate*, *8*(3), 550–568. https://doi.org/10.1175/1520-0442(1995)008<0550:CLTFAC>2.0.CO;2

Pye, H. O. T., Nenes, A., Alexander, B., Ault, A. P., Barth, M. C., Clegg, S. L., et al. (2020). The acidity of atmospheric particles and clouds. *Atmospheric Chemistry and Physics*, *20*(8), 4809–4888. https://doi.org/10.5194/acp-20-4809-2020

Qin, M., Wang, X., Hu, Y., Huang, X., He, L., Zhong, L., et al. (2015). Formation of particulate sulfate and nitrate over the Pearl River Delta in the fall: Diagnostic analysis using the community multiscale air quality model. *Atmospheric Environment*, *112*, 81–89. https://doi.org/10.1016/j.atmosenv.2015.04.027

Restad, K., Isaksen, I. S. A., & Berntsen, T. K. (1998). Global distribution of sulphate in the troposphere: A three-dimensional model study. *Atmospheric Environment*, *32*(20), 3593–3609. https://doi.org/10.1016/S1352-2310(98)00081-8

Román-Cascón, C., Yagüe, C., Sastre, M., Maqueda, G., Salamanca, F., & Viana, S. (2012). Observations and WRF simulations of fog events at the Spanish Northern Plateau. *Advances in Science and Research*, *8*(1), 11–18. https://doi.org/10.5194/asr-8-11-2012

Russell, A. G., & Brunekreef, B. (2009). A focus on particulate matter and health. *Environmental Science & Technology*, *43*(13), 4620–4625. https://doi.org/10.1021/es9005459

Schell, B., Ackermann, I. J., Hass, H., Binkowski, F. S., & Ebel, A. (2001). Modeling the formation of secondary organic aerosol within a comprehensive air quality model system. *Journal of Geophysical Research*, *106*(D22), 28275–28293. https://doi.org/10.1029/2001JD000384

Sha, T., Ma, X., Jia, H., van der A, R. J., Ding, J., Zhang, Y., & Chang, Y. (2019). Exploring the influence of two inventories on simulated air pollutants during winter over the Yangtze River Delta. *Atmospheric Environment*, *206*, 170–182. https://doi.org/10.1016/j.atmosenv.2019.03.006

Sha, T., Ma, X., Wang, J., Tian, R., Zhao, J., Cao, F., & Zhang, Y.-L. (2022). Improvement of inorganic aerosol component in $PM_{2.5}$ by constraining aqueous-phase formation of sulfate in cloud with satellite retrievals: WRF-Chem simulations. *Science of the Total Environment*, *804*, 150229. https://doi.org/10.1016/j.scitotenv.2021.150229

Song, S., Gao, M., Xu, W., Shao, J., Shi, G., Wang, S., et al. (2018). Fine-particle pH for Beijing winter haze as inferred from different thermodynamic equilibrium models. *Atmospheric Chemistry and Physics*, *18*(10), 7423–7438. https://doi.org/10.5194/acp-18-7423-2018

Sorooshian, A., Lu, M.-L., Brechtel, F. J., Jonsson, H., Feingold, G., Flagan, R. C., & Seinfeld, J. H. (2007). On the source of organic acid aerosol layers above clouds. *Environmental Science & Technology*, *41*(13), 4647–4654. https://doi.org/10.1021/es0630442

Sun, Y., Chen, C., Zhang, Y., Xu, W., Zhou, L., Cheng, X., et al. (2016). Rapid formation and evolution of an extreme haze episode in Northern China during winter 2015. *Scientific Reports*, *6*(1), 27151. https://doi.org/10.1038/srep27151

Tao, W., Su, H., Zheng, G., Wang, J., Wei, C., Liu, L., et al. (2020). Aerosol pH and chemical regimes of sulfate formation in aerosol water during winter haze in the North China Plain. *Atmospheric Chemistry and Physics*, *20*(20), 11729–11746. https://doi.org/10.5194/acp-20-11729-2020

The NCAR Command Language, Version 6.6.2. (2019). The NCAR Command Language, version 6.6.2 [Software]. UCAR/NCAR/CISL/TDD. https://doi.org/10.5065/D6WD3XH5

Wang, G., Zhang, R., Gomez, M. E., Yang, L., Levy Zamora, M., Hu, M., et al. (2016). Persistent sulfate formation from London Fog to Chinese haze. *Proceedings of the National Academy of Sciences of the United States of America*, *113*(48), 13630–13635. https://doi.org/10.1073/pnas.1616540113

Wang, J., Li, J., Ye, J., Zhao, J., Wu, Y., Hu, J., et al. (2020). Fast sulfate formation from oxidation of SO_2 by NO_2 and HONO observed in Beijing haze. *Nature Communications*, *11*(1), 2844. https://doi.org/10.1038/s41467-020-16683-x

Wang, L., Zhang, N., Liu, Z., Sun, Y., Ji, D., & Wang, Y. (2014). The influence of climate factors, meteorological conditions, and boundary-layer structure on severe haze pollution in the Beijing-Tianjin-Hebei region during January 2013. *Advances in Meteorology*, *2014*, 685971–685986. https://doi.org/10.1155/2014/685971

Wang, S., Zhou, S., Tao, Y., Tsui, W. G., Ye, J., Yu, J. Z., et al. (2019). Organic peroxides and sulfur dioxide in aerosol: Source of particulate sulfate. *Environmental Science & Technology*, *53*(18), 10695–10704. https://doi.org/10.1021/acs.est.9b02591

Wang, T., Liu, M., Liu, M., Song, Y., Xu, Z., Shang, F., et al. (2022). Sulfate Formation apportionment during winter haze events in North China. *Environmental Science & Technology*, *56*(12), 7771–7778. https://doi.org/10.1021/acs.est.2c02533

Wang, W., Liu, M., Wang, T., Song, Y., Zhou, L., Cao, J., et al. (2021). Sulfate formation is dominated by manganese-catalyzed oxidation of SO_2 on aerosol surfaces during haze events. *Nature Communications*, *12*(1), 1993. https://doi.org/10.1038/s41467-021-22091-6

Wang, X., Gemayel, R., Hayeck, N., Perrier, S., Charbonnel, N., Xu, C., et al. (2020). Atmospheric photosensitization: A new pathway for sulfate formation. *Environmental Science & Technology*, *54*(6), 3114–3120. https://doi.org/10.1021/acs.est.9b06347

Wang, X., Wei, W., Cheng, S., Yao, S., Zhang, H., & Zhang, C. (2019). Characteristics of $PM_{2.5}$ and SNA components and meteorological factors impact on air pollution through 2013–2017 in Beijing, China. *Atmospheric Pollution Research*, *10*(6), 1976–1984. https://doi.org/10.1016/j.apr.2019.09.004

Wonaschuetz, A., Sorooshian, A., Ervens, B., Chuang, P. Y., Feingold, G., Murphy, S. M., et al. (2012). Aerosol and gas re-distribution by shallow cumulus clouds: An investigation using airborne measurements. *Journal of Geophysical Research*, *117*(D17). https://doi.org/10.1029/2012JD018089

Wu, P., Ding, Y., & Liu, Y. (2017). Atmospheric circulation and dynamic mechanism for persistent haze events in the Beijing–Tianjin–Hebei region. *Advances in Atmospheric Sciences*, *34*(4), 429–440. https://doi.org/10.1007/s00376-016-6158-z

Yang, Y., Hu, X.-M., Gao, S., & Wang, Y. (2019). Sensitivity of WRF simulations with the YSU PBL scheme to the lowest model level height for a sea fog event over the Yellow Sea. *Atmospheric Research*, *215*, 253–267. https://doi.org/10.1016/j.atmosres.2018.09.004

Yao, M., Zhao, Y., Hu, M., Huang, D., Wang, Y., Yu, J. Z., & Yan, N. (2019). Multiphase reactions between secondary organic aerosol and sulfur dioxide: Kinetics and contributions to sulfate formation and aerosol aging. *Environmental Science and Technology Letters*, *6*(12), 768–774. https://doi.org/10.1021/acs.estlett.9b00657

Ye, C., Lu, K., Song, H., Mu, Y., Chen, J., & Zhang, Y. (2023). A critical review of sulfate aerosol formation mechanisms during winter polluted periods. *Journal of Environmental Sciences*, *123*, 387–399. https://doi.org/10.1016/j.jes.2022.07.011

Zhang, F., Wang, Y., Peng, J., Chen, L., Sun, Y., Duan, L., et al. (2020). An unexpected catalyst dominates formation and radiative forcing of regional haze. *Proceedings of the National Academy of Sciences of the United States of America*, *117*(8), 3960–3966. https://doi.org/10.1073/pnas.1919343117

Zhang, R., Li, Q., & Zhang, R. (2014). Meteorological conditions for the persistent severe fog and haze event over eastern China in January 2013. *Science China Earth Sciences*, *57*(1), 26–35. https://doi.org/10.1007/s11430-013-4774-3

Zhang, R., Sun, X., Shi, A., Huang, Y., Yan, J., Nie, T., et al. (2018). Secondary inorganic aerosols formation during haze episodes at an urban site in Beijing, China. *Atmospheric Environment*, *177*, 275–282. https://doi.org/10.1016/j.atmosenv.2017.12.031

Zhao, C., Yang, Y., Fan, H., Huang, J., Fu, Y., Zhang, X., et al. (2019). Aerosol characteristics and impacts on weather and climate over the Tibetan Plateau. *National Science Review*, *7*(3), 492–495. https://doi.org/10.1093/nsr/nwz184

Zheng, G. J., Duan, F. K., Su, H., Ma, Y. L., Cheng, Y., Zheng, B., et al. (2015). Exploring the severe winter haze in Beijing: The impact of synoptic weather, regional transport and heterogeneous reactions. *Atmospheric Chemistry and Physics*, *15*(6), 2969–2983. https://doi.org/10.5194/acp-15-2969-2015

Zhou, L., Liang, Z., Mabato, B. R. G., Cuevas, R. A. I., Tang, R., Li, M., et al. (2023). Sulfate formation via aerosol-phase SO_2 oxidation by model biomass burning photosensitizers: 3, 4-dimethoxybenzaldehyde, vanillin and syringaldehyde using single-particle mixing-state analysis. *Atmospheric Chemistry and Physics*, *23*(9), 5251–5261. https://doi.org/10.5194/acp-23-5251-2023

Zhou, Q., Zhang, Y., Jia, S., Jin, J., Lv, S., & Li, Y. (2020). Climatology of cloud vertical structures from long-term high-resolution radiosonde measurements in Beijing. *Atmosphere*, *11*(4), 401. https://doi.org/10.3390/atmos11040401

References From the Supporting Information

Boyce, S. D., & Hoffmann, M. R. (1984). Kinetics and mechanism of the formation of hydroxymethanesulfonic acid at low pH. *The Journal of Physical Chemistry*, *88*(20), 4740–4746. https://doi.org/10.1021/j150664a059

Gen, M., Liang, Z., Zhang, R., Go Mabato, B. R., & Chan, C. K. (2022). Particulate nitrate photolysis in the atmosphere. *Environmental Sciences: Atmosphere*, *2*(2), 111–127. https://doi.org/10.1039/D1EA00087J

Hoffmann, M., & Calvert, J. (1985). *Chemical transportation modules for eulerian acid deposition models, vol. II, the aqueous-phase chemistry*. U.S. Environmental Protection Agency.

Huang, X., Song, Y., Zhao, C., Li, M., Zhu, T., Zhang, Q., & Zhang, X. (2014). Pathways of sulfate enhancement by natural and anthropogenic mineral aerosols in China. *Journal of Geophysical Research: Atmospheres*, *119*(24), 14165–114179. https://doi.org/10.1002/2014JD022301

Ibusuki, T., & Takeuchi, K. (1987). Sulfur dioxide oxidation by oxygen catalyzed by mixtures of manganese(II) and iron(III) in aqueous solutions at environmental reaction conditions. *Atmospheric Environment*, *21*(7), 1555–1560. https://doi.org/10.1016/0004-6981(87)90317-9

Lagrange, J., Pallares, C., & Lagrange, P. (1994). Electrolyte effects on aqueous atmospheric oxidation of sulphur dioxide by ozone. *Journal of Geophysical Research*, *99*(D7), 14595–14600. https://doi.org/10.1029/94JD00573

Lee, Y. N., & Schwartz, S. E. (1982). In *Kinetics of oxidation of aqueous sulfur (IV) by nitrogen dioxide*. Elsevier.

Maass, F., Elias, H., & Wannowius, K. J. (1999). Kinetics of the oxidation of hydrogen sulfite by hydrogen peroxide in aqueous solution: Ionic strength effects and temperature dependence. *Atmospheric Environment*, *33*(27), 4413–4419. https://doi.org/10.1016/S1352-2310(99)00212-5

Martin, L. R., & Hill, M. W. (1987). The effect of ionic strength on the manganese catalyzed oxidation of sulfur(IV). *Atmospheric Environment*, *21*(10), 2267–2270. https://doi.org/10.1016/0004-6981(87)90361-1

Martin, L. R., Hill, M. W., Tai, A. F., & Good, T. W. (1991). The iron catalyzed oxidation of sulfur(IV) in aqueous solution: Differing effects of organics at high and low pH. *Journal of Geophysical Research*, *96*(D2), 3085–3097. https://doi.org/10.1029/90JD02611

Siefert, R. L., Johansen, A. M., Hoffmann, M. R., & Pehkonen, S. O. (1998). Measurements of trace metal (Fe, Cu, Mn, Cr) oxidation states in fog and stratus clouds. *Journal of the Air and Waste Management Association*, *48*(2), 128–143. https://doi.org/10.1080/10473289.1998.10463659